Zoosyst. Evol. 94 (1) 2018, 147–161 | DOI 10.3897/zse.94.21754

PENSOFT museum für naturkunde

Description of a new species of *Homonota* (Reptilia, Squamata, Phyllodactylidae) from the central region of northern Paraguay

Pier Cacciali[1,2,3], Mariana Morando[4], Luciano J. Avila[4], Gunther Köhler[1,2]

1 *Senckenberg Forschungsinstitut und Naturmuseum, Senckenberganlage 25, 60325 Frankfurt a.M., Germany*
2 *Johann Wolfgang Goethe-University, Institute for Ecology, Evolution & Diversity, Biologicum, Building C, Max-von-Laue-Straße 13, 60438 Frankfurt am Main, Germany*
3 *Instituto de Investigación Biológica del Paraguay, Del Escudo 1607, 1425 Asunción, Paraguay*
4 *Grupo de Herpetología Patagónica, IPEEC-CENPAT-CONICET. Puerto Madryn, Chubut, Argentina*

http://zoobank.org/207FF499-30F7-4465-B80E-3C0BD007D4E2

Corresponding author: *Pier Cacciali* (pier_cacciali@yahoo.com)

Received 19 October 2017
Accepted 15 February 2018
Published 28 February 2018

Academic editor:
Johannes Penner

Key Words

Dry Chaco
Gekkota
phylogeny
South America
taxonomy

Abstract

Homonota is a gecko distributed in central and southern South America with 12 species allocated in three groups. In this work, we performed molecular and morphological analyses of samples of *Homonota* from the central region of northern Paraguay, comparing the data with those of related species of the group: *H. horrida* and *H. septentrionalis*. We found strong molecular evidence (based on 16S, Cyt-b, and PRLR gene sequences) to distinguish this lineage as a new species. Morphological statistical analysis showed that females of the three species are different in metric characters (SVL and TL as the most contributing variables), whereas males are less differentiated. No robust differences were found in meristic characters. The most remarkable trait for the diagnosis of the new species is the presence of well-developed keeled tubercles on the sides of the neck, and lack of a white band (crescent-shaped) in the occipital area, which is present in *H. horrida* and *H. septentrionalis*. Nevertheless, in our sample, we found three specimens (one juvenile and two young adults) that exhibit the white occipital band. Thus, this character seems only reliable in adults of the new species. The new species is parapatric to *H. septentrionalis*, both inhabiting the Dry Chaco of Paraguay.

Introduction

Homonota is a gecko, inhabiting mainly xeric and rocky areas in central and southern South America (Cei 1993, Avila et al. 2012), with *Homonota darwinii* reaching the most austral distribution of the genus at 54° latitude south (Morando et al. 2014). Most of the species in the genus are nocturnal, although *H. uruguayensis* can be either diurnal or nocturnal (Carreira et al. 2005). *Homonota horrida* (Burmeister 1861), distributed in Argentina and Paraguay, was the second described species of the genus, after the controversial *H. fasciata* (Duméril and Bibron 1836). This latter species was described from "Martinique", a Caribbean island located out of the distribution of the southern cone Neotropical genus. Both species were considered synonyms by Abdala and Lavilla (1993), which was followed by posterior researchers until recently when Cacciali et al. (2017) found that the type specimen of *H. fasciata* is distinct from the types of *H. horrida*, and recognized them as different taxa. Currently, both species are considered valid, although *H. fasciata* remains a *species inquirenda* because of the lack of information on its distribution and uncertainty in its diagnostic characters (Cacciali et al. 2017). The most recently described species of the genus was *H. septentrionalis* Cacciali, Morando, Medina, Köhler, Motte & Avila, 2017, which is present in the western part of the Dry Chaco (western Paraguay and southern Bolivia). Three groups are currently recognized: *whitii* group composed of *H. whitii* Boulenger, 1885, *H. darwinii* Boulenger, 1885, *H. andicola* Cei, 1978, and *H. williamsii* Avila, Pérez, Minoli & Morando, 2012; *borelli* group with *H. borellii*

(Peracca, 1897), *H. uruguayensis* (Vaz-Ferreira & Sierra de Soriano, 1961), *H. rupicola* Cacciali, Ávila & Bauer, 2007, and *H. taragui* Cájade, Etchepare, Falcione, Barrasso & Álvarez, 2013; and the *horrida* group (indicated as *fasciata* group by Morando et al. 2014) which contains *H. horrida* (Burmeister, 1861), *H. underwoodi* Kluge, 1964, and *H. septentrionalis* Cacciali, Morando, Medina, Köhler, Motte & Avila, 2017. Cacciali et al. (2017) suggested that more revisions are needed to understand the true taxonomic status of *H. fasciata* because currently it is not possible to know to which group it belongs and it is considered *incertae sedis*.

Four species of *Homonota* are recorded in Paraguay: *H. borellii*, *H. rupicola*, *H. horrida*, and *H. septentrionalis*. The most commonly known species was *Homonota horrida* recorded for the "Chaco" (Kluge 1964, Talbot 1978, 1979). Even after the synonymy of *H. horrida* with *H. fasciata* (Abdala and Lavilla 1993) the name *H. horrida* was still used in Paraguayan reports (Aquino et al. 1996, Ziegler et al. 2002). Many specimens of *H. septentrionalis* were referred to as *H. horrida* (those from the westernmost part of the Paraguayan Chaco) according to Cacciali et al. (2017). *Homonota rupicola* is an endemic species found in a rocky hill, east of the Paraguay River; and *H. borellii* was recorded from a few specimens from "Defensores del Chaco" and "Médanos del Chaco" National Parks (Cacciali et al. 2016). Thus, most of the species of *Homonota* from Paraguay are present in the Chaco, which is part of the "Dry Diagonal" formed by Caatinga, Cerrado, and Chaco, characterized by dry seasonal woodlands (Prado and Gibbs 1993). In Paraguay the Chaco is divided in two ecoregions: Humid Chaco and Dry Chaco, and most of the *Homonota* samples are located in the latter (Cacciali et al. 2016).

After the description of *H. septentrionalis*, the same authors continued to study and analyze the taxonomy of Paraguayan samples of *Homonota* from the Chaco, within the framework of a barcoding initiative of the herpetofauna from Paraguay. We performed genetic and morphological analyses among different populations of *Homonota* from the central region of northern Paraguay. Based on genetic and morphological differences, and applying a species delimitation algorithm, we found enough differences to consider these new samples as a different taxonomic unit from those previously recorded for Paraguay. We present here a detailed analysis along with the description of this new species.

Methods

We extracted DNA from three samples of *Homonota* from the central area of northern Paraguay (Occidental Region), which were compared with available sequences of the remaining members of the genus (except *H. fasciata*) to assess its taxonomic relationships in the gene tree. We sequenced fragments of mitochondrial genes rRNA 16S and Cytochrome b (Cytb) and the nuclear gene prolactine receptor (PRLR). Samples used and GenBank accession numbers are specified in Table 1. Samples of 16S were available only for the *horrida* group. To root the tree we included two outgroups (*Garthia gaudichaudii* and *Phyllopezus przewalskii* (Table 1) based on Morando et al. (2014).

Tissue samples were first washed for 15 h with 50 ml Phosphate-buffered saline (PBS) (diluted of 1:9 PBS: H_2O). The DNA extraction was carried out with the DNeasey kit of Qiagen. We used 25 µl of reaction mix for every sample for the PCR (except for PRLR where we used 20 µl). Reagents and concentrations for the PCR mix for the amplification of every gene, are provided in Suppl. material 1: Appendix S1. Primers (produced by Eurofins MWG Operon) used for amplification and sequencing, along with PCR conditions for each gene are detailed in Suppl. material 1: Appendix S2.

We used SeqTrace 0.9.0 (Stucky 2012) for examination of chromatograms and to generate the consensus sequences. We used MAFFT 7 (Katoh and Standley 2013) to automatically align the sequences through its webserver. For alignment of sequences of 16S, we included the Q-INS-i search strategy for corrections with the secondary structure of that gene (Katoh and Toh 2008). We used MSA Viewer (Yachdav et al. 2016) to visualize the alignments and export them to fasta format. We estimated the best substitution model for each gene (separately) with PartitionFinder2 (Lanfear et al. 2016) using the PhyML 3.0 algorithm (Guindon et al. 2010). We used the corrected Akaike Information Criterion (AICc) (Burnham and Anderson 2002) to select the best substitution model, but under the premise that it is not correct to use models that include both +G and +I (Sullivan et al. 1999, Mayrose et al. 2005). Then we chose the subsequent model in the best partition schemes when both were suggested by the AICc.

We performed two phylogenetic analyses, first using a Maximum Likelihood (ML) approach, and then a Bayesian inference (BI) to compare the trees topologies. These analyses were made for each gene individually and for a concatenated dataset of the three genes together. For the ML analysis we used IQ-Tree (Nguyen et al. 2015) through its webserver (Trifinopoulos et al. 2016) using 10,000 non parametric bootstrap replicates plus 10,000 replicates of Shimodaira-Hasegawa approximate likelihood ratio (SH-aLRT) (Anisimova et al. 2011) and 10,000 ultrafast bootstrap (UFBoot) approximation replicates (Minh et al. 2013). We converted the alignment to nexus format in the online server Alter (Glez-Peña et al. 2010) available at http://sing.ei.uvigo.es/ALTER/, to be used in MrBayes v3.2 (Huelsenbeck and Ronquist 2001, Ronquist and Huelsenbeck 2003) for a BI. For this, we ran the analysis in independent duplicates, each with 1,000,000 generations for MCMC with a sampling frequency of 500 generations. We visualized the trees and exported them using FigTree v1.4.3 (available at http://tree.bio.ed.ac.uk/software/figtree/). We considered convergence when the standard deviation of split frequencies was 0.015 or less and when the Potential Scale Reduction Factor approached 1.0 (Gelman and Rubin 1992).

Table 1. Specimens used for genetic analyses and GenBank accession numbers for every gene. Asterisks (*) indicate tissue samples without voucher. Numbers in bold are samples generated for this work.

Species	Voucher	16S	Cytb	PRLR	GenSeq Nomenclature
Homonota andicola	LJAMM-CNP 12493	MD	KJ484188	KJ484274	genseq-3
	LJAMM-CNP 12495	MD	KJ484189	KJ484275	genseq-3
Homonota borellii	LJAMM-CNP 12116	MD	KJ484205	KJ484276	genseq-4
	LJAMM-CNP 12119	MD	KM677796	MD	genseq-4
	LJAMM-CNP 12125	MD	KJ484206	KJ484277	genseq-4
Homonota darwinii	LJAMM-CNP 9266	MD	KJ484191	MD	genseq-3
	LJAMM-CNP 9813	MD	MD	KJ484278	genseq-3
	LJAMM-CNP 11424	MD	KJ484190	MD	genseq-3
Homonota horrida	BYU 47941	MF278828	KJ484192	**MG950402**	genseq-3
	LJAMM-CNP 10493	MD	KM677795	MD	genseq-3
	LJAMM-CNP 10495	MF278829	MD	**MG950403**	genseq-3
	LJAMM-CNP 10576	MF278830	MD	**MG950404**	genseq-3
	LJAMM-CNP 10577	MD	KJ484208	MD	genseq-3
Homonota rupicola	MNHNP-1*	MD	KJ484193	KJ484281	genseq-3
	MNHNP-2*	MD	KJ484194	KJ484282	genseq-3
Homonota septentrionalis	MNHNP 11406	MD	MF278843	MF278849	genseq-2
	MNHNP 11409	MD	MF278844	MF278850	genseq-2
	MNHNP 11873	MF278831	MD	**MG950405**	genseq-3
	MNHNP 12238	MF278832	MD	MD	genseq-1
	SMF 101984	MF278833	MD	**MG950406**	genseq-2
Homonota taragui	LJAMM-CNP 14419	MD	KJ484195	KJ484283	genseq-3
	LJAMM-CNP 14420	MD	KJ484196	KJ484284	genseq-3
Homonota underwoodi	LJAMM-CNP 10923	MD	KJ484197	KJ484286	genseq-4
	LJAMM-CNP 10931	MD	KJ484198	KJ484297	genseq-4
Homonota uruguayensis	UFRGS 2139	MD	MD	KJ484296	genseq-4
	UFRGS 5769	MD	KM677689	MD	genseq-4
	UFRGS 5770	MD	KM677690	MD	genseq-4
	UFRGS 5771	MD	KM677691	MD	genseq-4
Homonota whitii	LJAMM-CNP 14387	MD	KJ484199	MD	genseq-4
	LJAMM-CNP 14388	MD	KJ484200	MD	genseq-4
Homonota williamsii	LJAMM-CNP 4467	MD	KJ484201	KJ484287	genseq-3
	LJAMM-CNP 6517	MD	KJ484202	KJ484288	genseq-2
Homonota sp. n.	SMF 101436	MD	**MG950409**	**MG950407**	genseq-2
	SMF 101438	**MG947388**	**MG950410**	**MG950408**	genseq-2
	SMF 101439	MD	**MG950411**	MD	genseq-2
Outgroups					
Garthia gaudichaudii	E61214	MD	FJ985045	MD	
	IBE_G1(1)	MD	MD	KJ484289	
Phyllopezus przewalskii	LG1093	JN935567	JQ826890	JQ825640	
	LJAMM-CNP 12089	MD	KJ484203	MF278849	

When frequencies did not converge we continued adding 500,000 generations until convergence was achieved.

We assessed the degree of intraspecific divergence within the alignment (removing the outgroups) with the species delimitation test ABGD (Puillandre et al. 2012) through its webserver (http://wwwabi.snv.jussieu.fr/public/abgd/abgdweb.html), using 10 steps of prior minimum and maximum simple genetic distance from 0.001 to 0.1 (default), and 0.5 of relative gap width, since higher (default) values tend to exceedingly split clades (Kekkonen et al. 2015, Yang et al. 2016). For this analysis we used only Cytb which was the mitochondrial gene better represented in our samples, and available for all the species within the genus. The last step using genetic data was the assessment of a species tree based on the clustering proposed by the species delimitation test. To do this we used *BEAST (Drummond et al. 2012) in BEAST 2.4.7 (Ogilvie et al. 2017) under 1,000,000 generations for the mcmc model, visualizing the posterior probability in DensiTree 2.2.6 (Bouckaert et al. 2014).

Additionally, we generated morphological data for 13 specimens (7 males and 6 females) of the new species and

taxa with similar pattern (related taxa of the *horrida* group) looking for potential diagnostic characters. Thus, we used for comparison *H. horrida* (7 males and 5 females) and *H. septentrionalis* (10 males and 12 females), using standard variables (continuous data expressed in mm) already used by Avila et al. (2012) and Cacciali et al. (2017):

SVL snout–vent length, from tip of snout to vent.
TrL trunk length, distance from axilla to groin from posterior edge of forelimb insertion to anterior edge of hind limb insertion.
FL foot length, from the tip of the claw of the 4th straightened toe to the back of the heel.
TL tibial length, measured between the level of the knee and the level of the heel, as shown by Köhler (2014).
AL arm length, from tip of claws of the 3rd finger to elbow.
HL head length, distance between anterior edge of auditory meatus and snout tip.
HW head width, taken at the level of the temporal region, corresponding to the widest part of the head.
HH head height, maximum height of head, at level of parietal area.
END eye–nostril distance, from the anterior edge of the eye to the posterior edge of the nostril.
ESD eye–snout distance, from the anterior edge of the eye to the tip of the snout.
EMD eye–meatus distance, from the posterior edge of the eye to the anterior border of the ear opening.
ID interorbital distance, shortest distance between orbits.
IND internostril distance, shortest distance between nares.
DT number of keeled dorsal tubercles from occipital area to cloaca level.
TVS number of transversal rows of ventral scales, counted longitudinally at midline from the chest (shoulder level) to inguinal level.
LVS number of longitudinal rows of ventral scales, counted transversally at midbody.
SL number of supralabial scales.
IL number of infralabial scales.
4TL number of lamellae under the fourth toe.
3FL number of lamellae under the third finger.

Measurements were taken with digital calipers (precision 0.01), but only the first decimal considered to limit discrepancies. For the morphological analyses only specimens of ~40 mm or larger were included. When paired structures exist, data are presented in left/right orientation, and only the left side was used for statistical analyses. In the color descriptions, the capitalized colors and the color codes (in parentheses) are those of Smithe (1981) for live animals and Köhler (2012) for preserved specimens.

We compared the morphological variation among species through a discriminant function analysis (DFA), testing the normality of the variables with a Shapiro-Wilk (*W*) test (Shapiro et al. 1968, Zar 1999), and for the DFA we only used variables that were normally distributed. We used PAST 3.14 (Hammer et al. 2001) to perform these tests. Meristic (discrete) and metric (continuous) data were analyzed separately. Examined specimens are detailed in Appendix 1. We present a table of localities of the specimens examined in Suppl. material 1: Appendix S3.

Results

The final alignments of 16S, Cytb, and PRLR consisted of 539, 793, and 457 bp, respectively. Alignments and trees are available at TreeBASE (ID: 22305). The best substitution model for 16S was GTR+G, for Cytb TVM+I(1stpos)|TIM+G(2ndpos)|SYM+G(3rdpos), and for PRLRK81(1stpos)|GTR+G(2nd+3rdpos). The complete table with scores is provided in Suppl. material 1: Appendix S4. The topology of the ML (Suppl. material 1: Fig. S1) and BI (Suppl. material 1: Fig. S2) trees using 16S coincide in recognizing three clusters, but the ML tree shows the new species as a sister clade to *H. septentrionalis*, whereas BI shows a trichotomy including *H. horrida*, *H. septentrionalis*, and the new species. Trees of ML and BI based on Cytb have the same topology (Suppl. material 1: Figs S3–S4), with strong support values. In these trees *H. andicola* and *H. whitii* are sister clades, as are *H. darwinii* and *H. williamsii*, and they are sister to the remaining *Homonota* species. The *borellii* group shows *H. uruguayensis* as sister to *H. borellii* + *H. rupicola* + *H. taragui*. Finally, within the *horrida* group, *H. underwoodi* appears as the sister to the remaining *Homonota* with banded coloration pattern. In this part of the tree *H. horrida* is rendered as sister to the clade *H. septentrionalis* plus the new taxon. The topologies of the ML and BI trees using PRLR are also the same (Suppl. material 1: Figs S5–S6). Species in the *whitii* group are clustered together, and the *borellii* group also shows monophyly but with a unresolved polytomy. In the *horrida* group *H. underwoodi* is also suggested as sister to the remaining species, with the new species and *H. septentrionalis* showing the most recent divergence. The trees using the concatenated dataset (with both ML and BI) show similar branch arrangement previously observed in trees of individual genes (Suppl. material 1: Figs S7–S8). Only two samples (UFRGS 2139 of *H. uruguayensis* and LJAMM-CNP 9813 of *H. darwinii*) are not allocated within their respective taxa, probably because some genes are lacking for some species.

The analysis of intraspecific genetic divergence with ABGD results in 12 groups (Suppl. material 1: Appendix S5), which represent nearly all described species (except *H. fasciata*) and the new species, providing evidence for its recognition as a distinct taxon. This is highly congruent with the clusters shown by the gene trees. The species tree shows consensus in the clusters of the three groups of the genus *Homonota*, with slight differences in the branch arrangements. The lower value (density of green lines in Figure 1) shows a trichotomy where the three groups are nested together, and with similar proba-

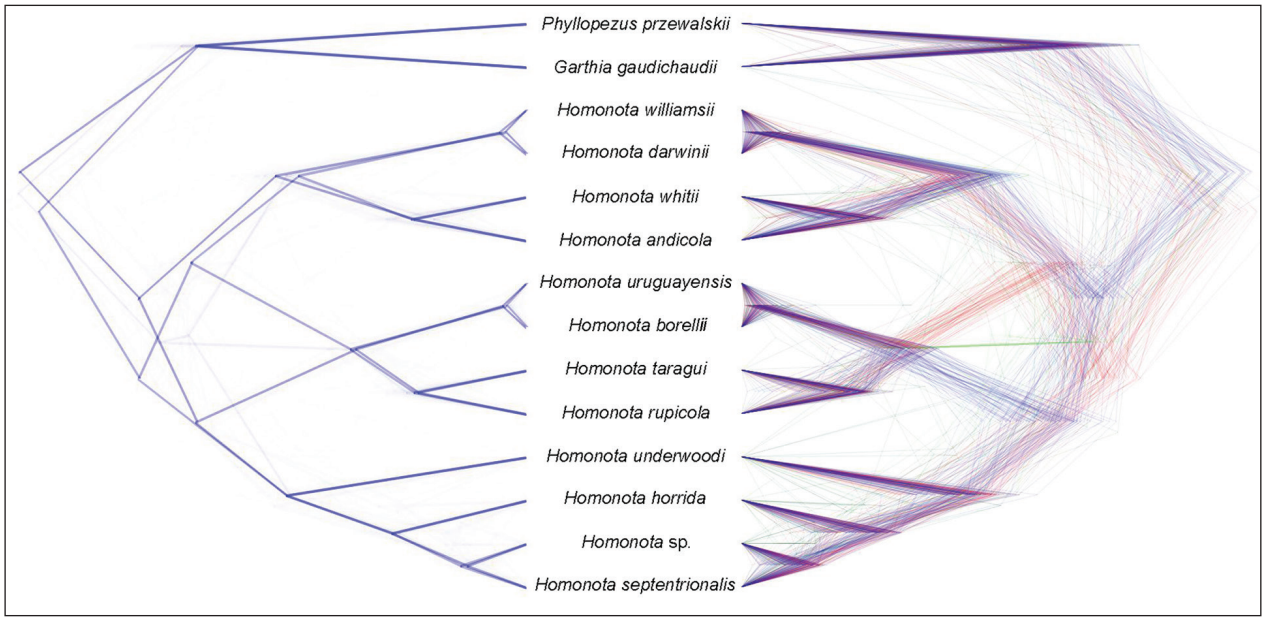

Figure 1. Species tree (left) and density of trees (right) for the species of the genus *Homonota*, based on the genes 16S, Cytb, and PRLR. The intensity in the color of the species tree is proportional to the probability.

Table 2. Normality Shapiro-Wilk (*W*) values for metric (above) and meristic (below) characters showing the *p* value. Values shaded in gray did not reach normality. See Methods section for reference to the acronyms.

	Continuous												
	SVL	TrL	FL	TL	AL	HL	HW	HH	END	ESD	EMD	ID	IND
W	0.978	0.979	0.957	0.987	0.982	0.979	0.976	0.983	0.979	0.967	0.969	0.975	0.952
p	0.503	0.506	0.087	0.849	0.696	0.575	0.401	0.758	0.555	0.199	0.284	0.400	0.050
	Discrete												
	DT	TVS	LVS	SL	IL	4TL	3FL						
W	0.962	0.971	0.965	0.779	0.788	0.913	0.948						
p	0.109	0.291	0.164	$3.05E^{-7}$	$4.65E^{-7}$	0.008	0.023						

bilities a species tree that clusters the *whitii* group as sister to the *borellii* group (density of red lines) and another where the *whitii* group is sister to the *borellii* group + *horrida* group (density of blue lines). Same as observed in the gene trees, *H. underwoodi* is presented as the sister clade to the remaining members of the group, and *H. horrida* sister to the new species of *Homonota* and *H. septentrionalis* with a rather deep divergence between these two taxa.

All continuous morphological variables had normal distributions (Table 2). The DFA for metric data showed that females of the three species are more differentiated than males (Fig. 2). The most contributing variables were SVL and TL for Axis 1, and SVL and TrL for Axis 2 and 3 (Table 3). Given the high eigenvalue of axes 1 and 2 (3.79 and 2.34 respectively, Fig. 2) suggests that the groups are significantly differentiated. For the meristic data, only DT, TVS, and LVS reached normality (Table 2), and DFA with these variables showed a high degree of overlapping without group discrimination and low eigenvalues (Fig. 3), and weak discrimination values (Table 3). Raw metric and meristic data are presented in Suppl. material 1: Tables S1 and S2.

Table 3. Most contributing continuous (Cont.) and discrete (Disc.) variables (highlighted in bold) for Axis 1–3 of the DFA.

	Variables	Axis 1	Axis 2	Axis 3
Cont.	SVL	**0,417**	**1,202**	**–3,447**
	TrL	–0,187	**0,690**	**–1,798**
	FL	0,132	0,401	–0,479
	TL	**0,228**	0,193	–0,417
	AL	0,201	0,213	–0,553
	HL	–0,017	0,357	–0,605
	HW	–0,128	0,218	–0,525
	HH	–0,199	0,187	–0,258
	END	–0,021	0,099	–0,193
	ESD	–0,052	0,111	–0,392
	EMD	0,144	0,134	–0,221
	ID	–0,028	–0,013	–0,302
	IND	0,002	0,127	–0,050
Disc.	DT	**1.424**	–1.232	**–1.338**
	TVS	**2.166**	**1.825**	0.921
	LVS	<0.001	**1.482**	**–1.255**

There is a strong molecular congruence in the recognition of 12 taxa within the genus *Homonota* (three of them with a banded coloration pattern), which added

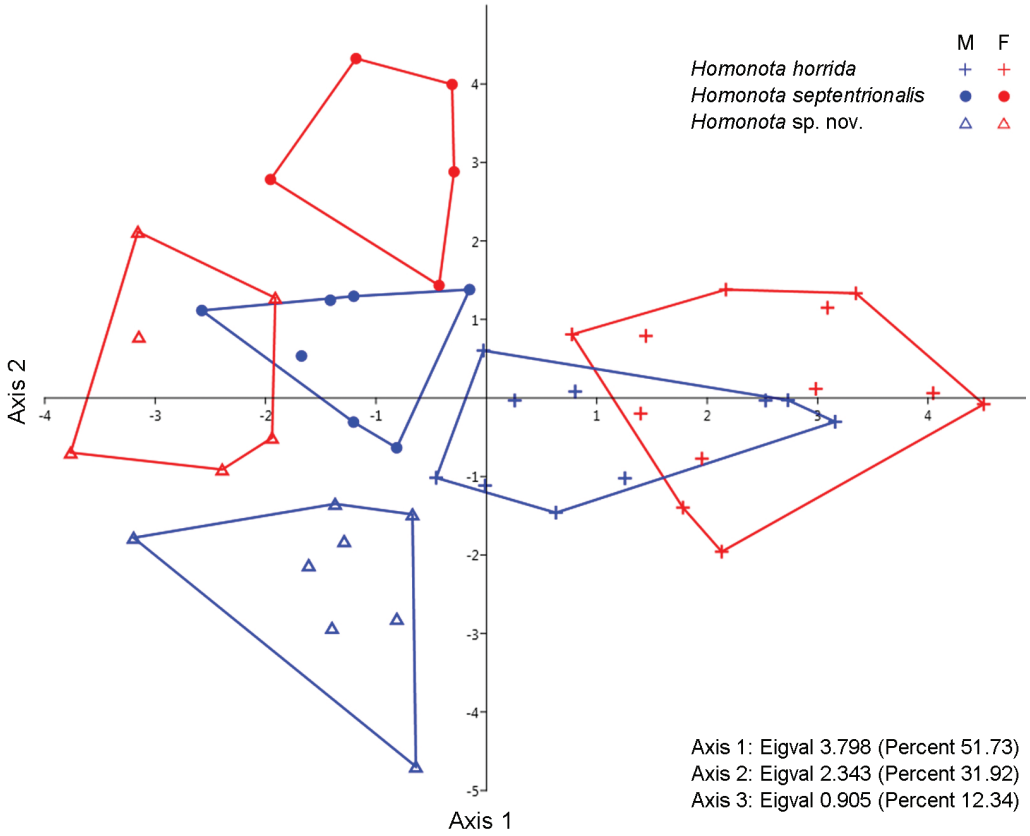

Figure 2. Discriminant Function Analysis scatter plot of individual scores for the three most informative axes for continuous variables of *Homonota horrida*, *H. septentrionalis*, and *Homonota* sp. n. Eigval: Eigenvalues. M: males. F: females.

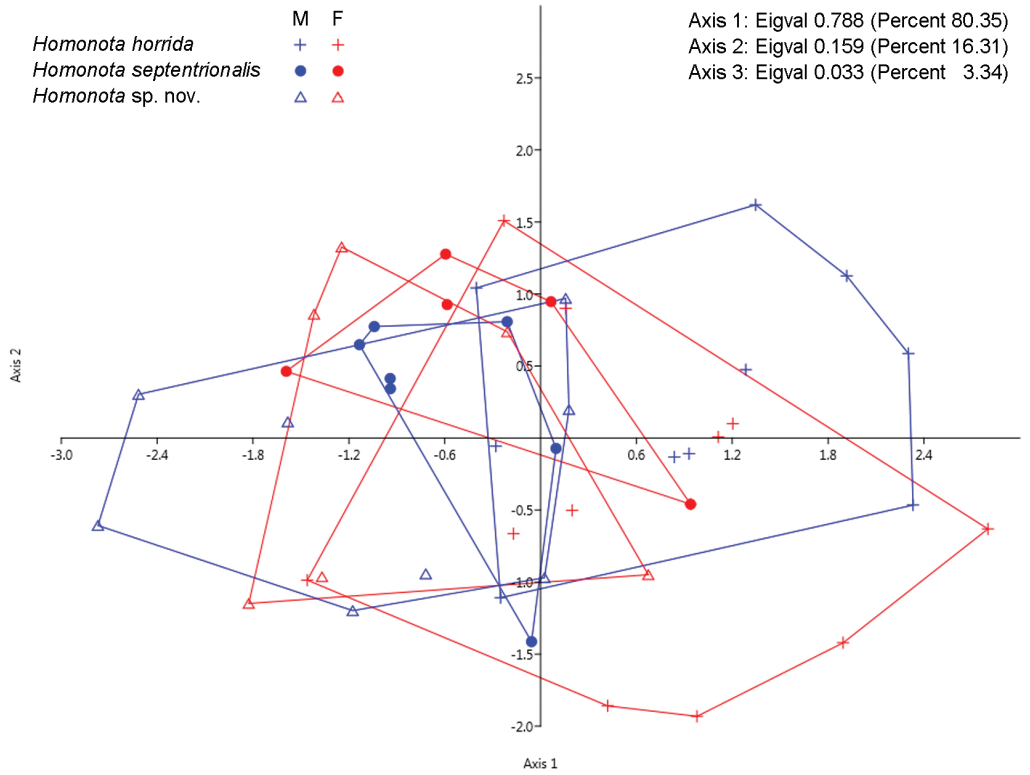

Figure 3. Discriminant Function Analysis scatter plot of individual scores for the three most informative axes for discrete variables of *Homonota horrida*, *H. septentrionalis*, and *Homonota* sp. n. Eigval: Eigenvalues. M: males. F: females.

to the significant differences among the three species with banded pattern based on the DFA, and the additional morphological distinctions discussed below are used to identify the new taxon described here.

Homonota marthae sp. n.

http://zoobank.org/FAB96653-46FF-4291-A23B-0FDB390AC54D

Holotype. SMF 101441 (field number GK-3783) (Fig. 4), adult female, collected on February 17th 2012 by Gunther Köhler in Dry Chaco, near the main house of Estancia Amistad (22.406°S, 60.728°W, elevation ca. 190 masl), Boquerón Department, Paraguay (Fig. 5).

Paratypes. Paraguay: Boquerón Department: Comunidad Ayoreo Jesudi (MNHNP 10744); Comunidad Ayoreo Tunucojai (MNHNP 10534); Estancia Amistad (SMF 101437); Estancia Jabalí (MNHNP 7832); Filadelfia (MNHNP 2795, 2798, 2810, 11790, 11791, 11793, SMF 101436, 101438–40, 101442); 31.5 km S Filadelfia (MNHNP 9726).

Diagnosis. A species of *Homonota* assigned to the *horrida* group given its relationship (based on molecular evidence) with *H. horrida*, and by the color pattern composed of a vertebral and five to seven transversal clear lines appearing as a banded *Homonota* smilar to *H. horrida* and *H. septentrionalis*. *Homonota marthae* has a robust body, and prominently keeled tubercles disposed in four to eight longitudinal rows on the dorsum.

Homonota marthae can be differentiated from all species in the genus, except *H. fasciata*, *H. horrida*, *H. darwinii*, and *H. septentrionalis* by the color pattern of transversal bands on the dorsum (reticulated pattern in the remaining species). *Homonota marthae* is further differ-

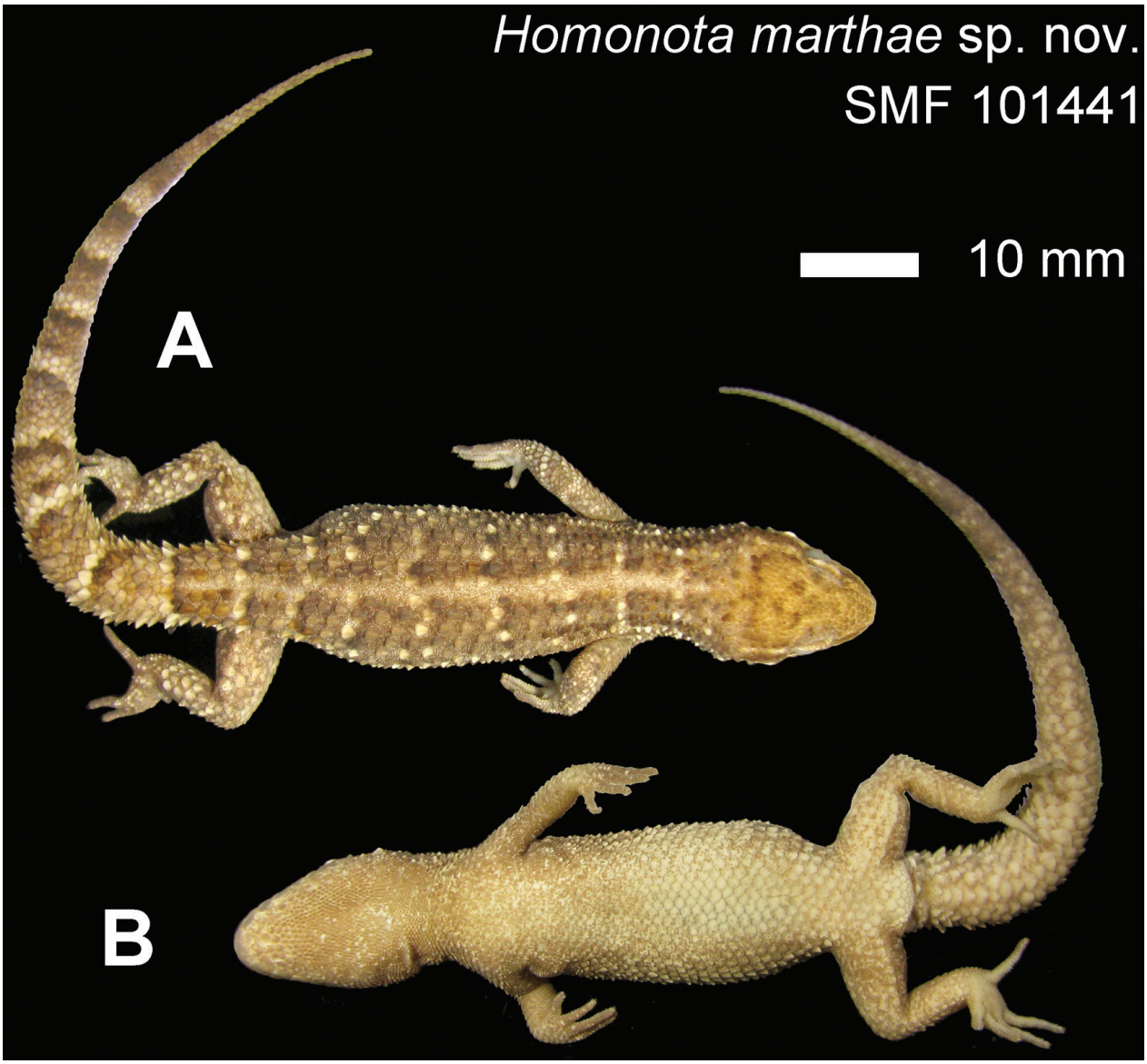

Figure 4. Dorsal (**A**) and ventral (**B**) views of the holotype of *Homonota marthae*.

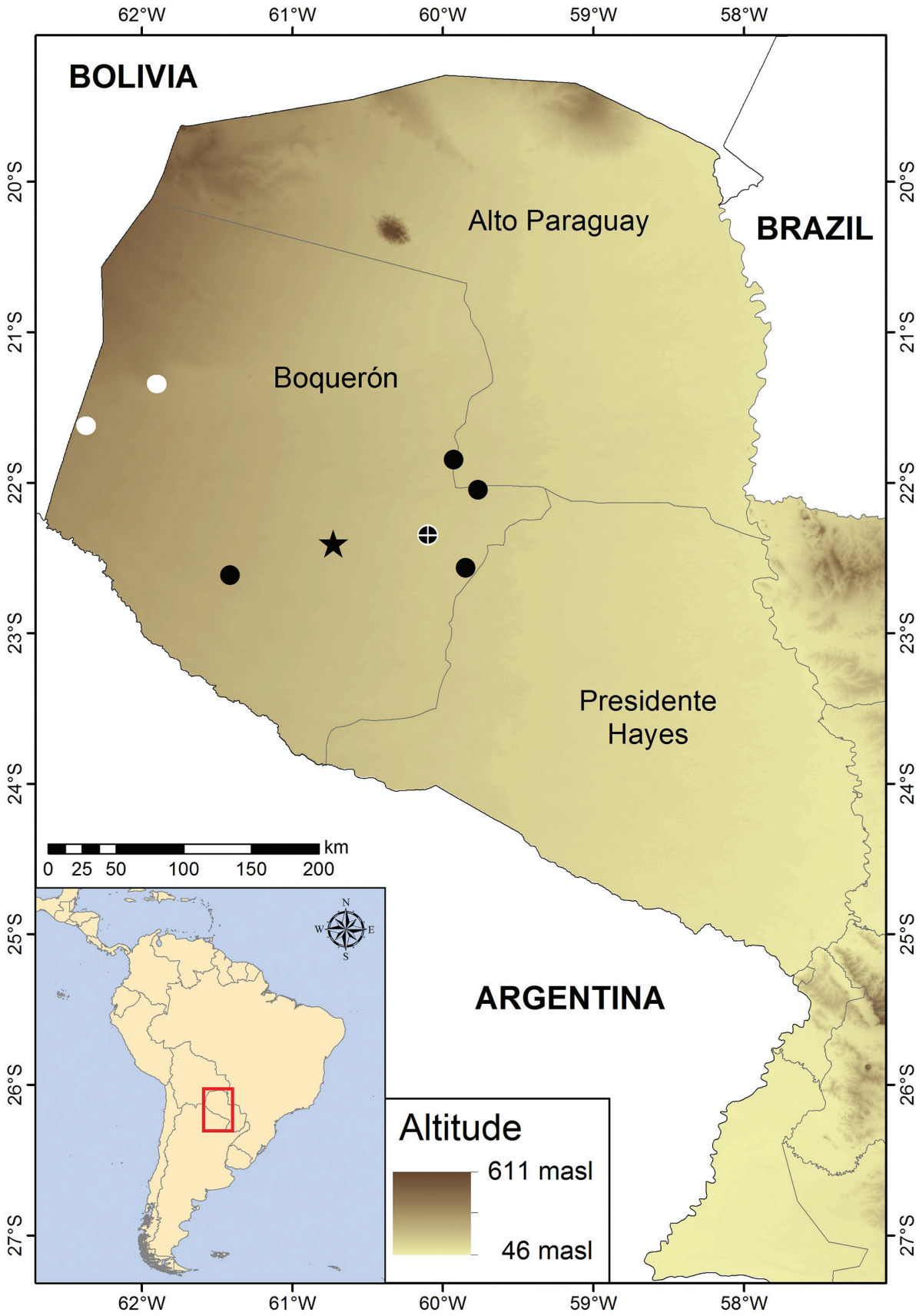

Figure 5. Occidental Region of Paraguay, indicating the political division, showing the known records for *Homonota septentrionalis* (white circles) and the analyzed records of *Homonota marthae* (black circles), and its type locality (star). Circle with a white cross, indicates origin of the genetic samples. High resolution elevation base map (30 seconds resolution) taken from Consortium for Spatial Information (CGIAR-CSI) available on http://www.diva-gis.org/gdata (Jarvis et al. 2008).

entiated from *H. andicola*, *H. whitii*, *H. darwinii*, and *H. underwoodi* by the keeled scales along the whole dorsum (vs. smooth dorsal scales in *H. andicola*, *H. whitii*, and *H. underwoodi*, and keeled scales restricted to the posterior part of the dorsum in *H. darwinii*). It differs from *H. fasciata* by having a serrated edge of the auditory meatus (vs. smooth anterior margin in *H. fasciata*); presence of one or two enlarged tubercles on the upper edge of the auditory meatus (vs. no enlarged tubercles in *H. fasciata*); and a smaller size of the postmental scales (vs. postmentals of the size of the first infralabials in *H. fasciata*). *Homonota marthae* differs from *H. horrida* by the higher position of the ear opening in relation to the level of the mouth (vs. lower positioned in *H. horrida*); from *H. septentrionalis* by more developed keeled tubercles on the sides of the neck (Fig. 6) (vs. less developed tubercles in *H. septentrionalis*). Finally, adults of *H. marthae* differ from these both species by the lack of a white band (usually crescent-shaped) on the occipital area (vs. white occipital crescent-shaped band present in *H. horrida* and *H. septentrionalis*) (Fig. 7). An artificial key for identification of the species of the genus is presented at the end of the work.

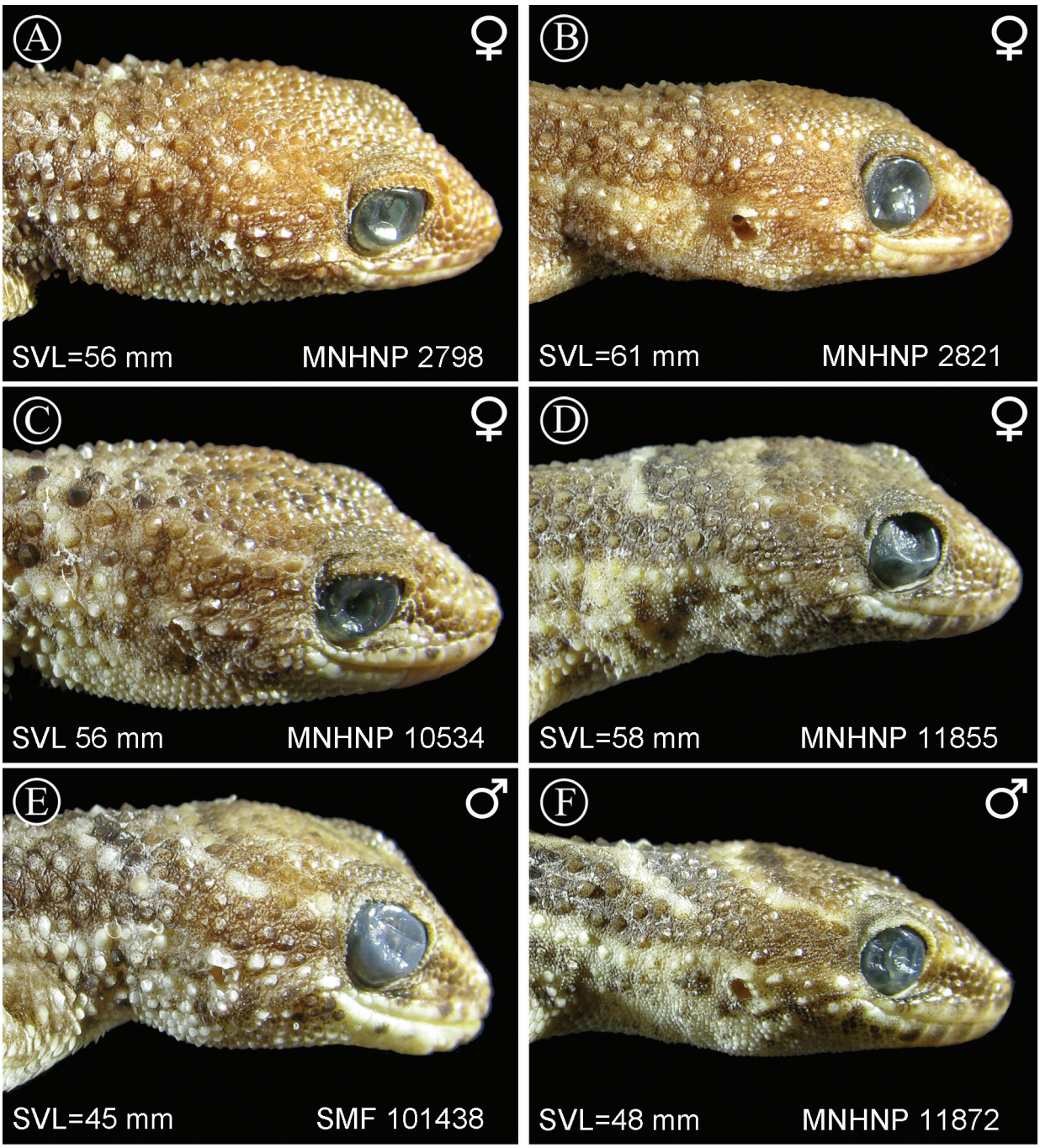

Figure 6. Plate showing the difference in scalation among individuals of similar sizes and same gender, of *Homonota marthae* (**A**, **C**, **E**) and *H. septentrionalis* (**B**, **D**, **F**). Note the more developed keeled tubercles on the sides of the neck in the former species.

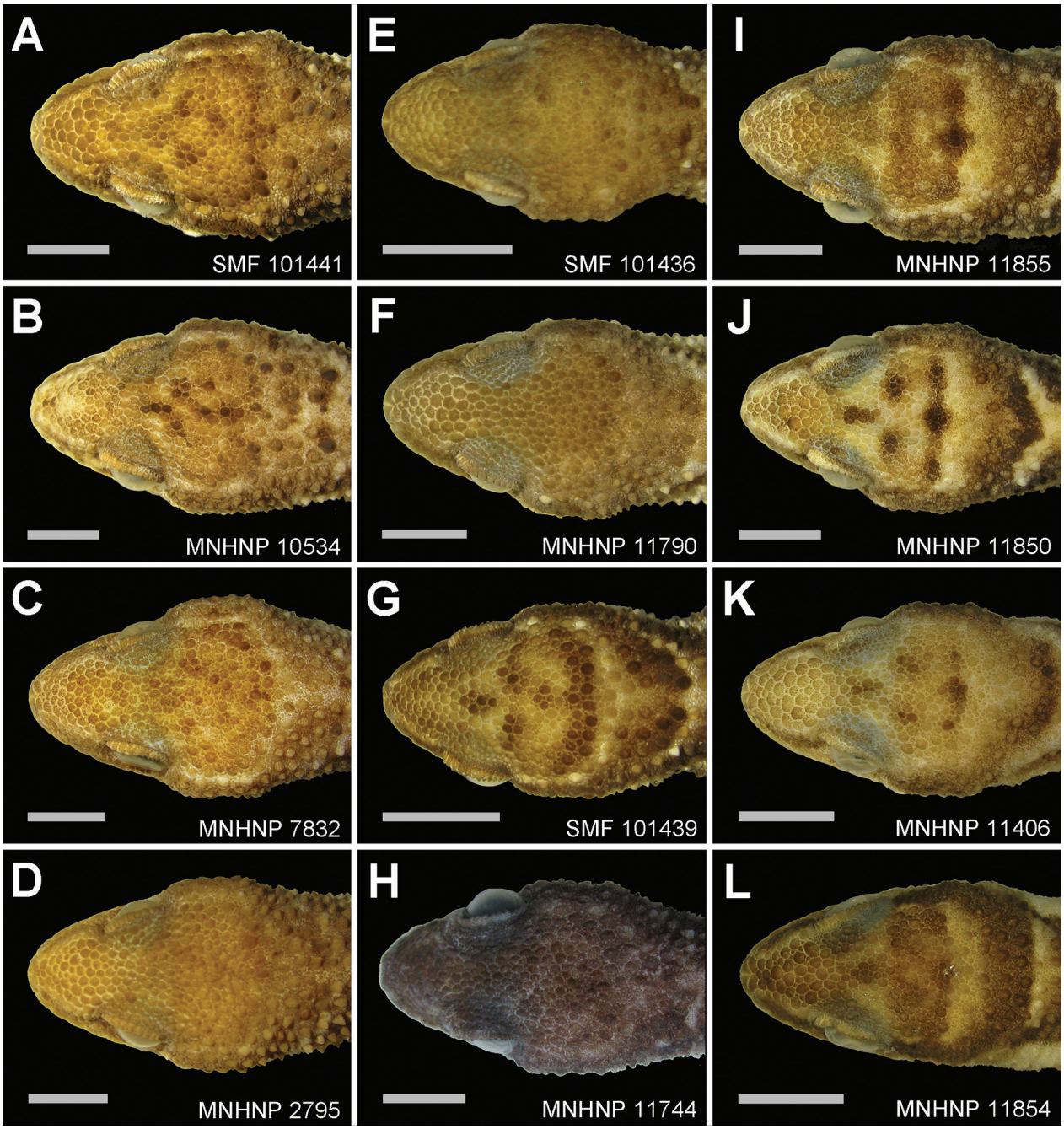

Figure 7. Variation in color patterns of *Homonota marthae* (**A**–**H**). The lack of the white occipital crescent-shaped line (present in *H. septentrionalis*, **I**–**L**) is evident in most of the specimens. Scale bars: 5 mm.

Description of the holotype. Adult female, SVL 56 mm (4.1 times the HL), TrL 26 mm, tail length 70 mm, FL 11.0 mm, TL 9.6 mm, AL 13.3 mm, HL 13.6 mm, HW 10.8 mm, HH 8.3 mm, END 4.2 mm, ESD 5.9 mm, EMD 4.7 mm, ID 4.6 mm, IND 2.0 mm; rostral wider (2.7 mm) than high (1.5 mm) with a median groove covering the upper two thirds of the scale; nares surrounded by rostral, supranasal, and postnasal; SL 8/8; one elongated tubercular scale on the mouth commissure; muzzle slightly convex, covered by large homogeneous juxtaposed scales; head covered with big homogeneous juxtaposed scales on the dorsal area, intermixed with small granules; superciliary scales imbricated, associated to spiny-like scales on the posterior half of the orbit; scales on lateral surface of the head heterogeneously covered with strongly conical tubercles intermixed with small granules; auditory meatus oblique and with serrated edge, and one large elongated scale on the upper border; IL 6/6, the last less than half the size of the others; mental bell-shaped; two postmentals less than twice the size of the following posterior scales, contacting the mental, the first IL, and four posterior scales; scales under the head gradually reducing in size posteriorly; dorsal and lateral parts of the neck with granular juxtaposed scales mixed with tubercles;

ventral side of the head covered by imbricate cycloid scales; body dorsally covered with 14–16 rows of strongly keeled scales, separated by one to two small granules in the pleural areas, and three to four granules in the vertebral area; ventral scales cycloid and imbricate arranged in 16 longitudinal rows at midbody; suprascapular, axillary, inguinal regions, and cloacal opening surrounded by small imbricate granules; anterior and dorsal surfaces of limbs covered by large imbricate scales, keeled on the dorsal surface; posterior region of limbs covered by small juxtaposed granules; ventral surface of forelimbs with juxtaposed granules, and ventral surface of hind limbs with large imbricate scales; subdigital lamellae of hands starting from pollex were recorded as follows: 8/8 – 10/12 – 15/13 – 16/16 – 11/11; subdigital lamellae of feet starting from hallux were recorded as follow: 15/13 – 19/17 – 15/16 – 12/12 – 9/9; tail with large imbricated and mucronate scales, 10–12 per caudal whorl.

Coloration of the holotype (in preservative). After five years in preservative, the coloration was recorded as follows: Head Mikado Brown (42) with Warm Sepia (40) speckling on the dorsal surface; Warm Sepia (40) on the sides, with a Light Buff (2) line from nares to orbit, and continuing behind the orbit above the temporal region; supralabials and infralabials Medium Neutral Gray (298) with suffusions of Smoky White (261); and Fawn Color (258) ventrally. Dorsal background color of the body Beige (254) with Vandyke Brown (282) splotches, and poorly defined Chamois (84) transversal lines; Drab (19) laterally, with Dusky Brown (285) and Pale Buff (1) splotches; and Ground Cinnamon (270) ventrally, with Smoky White (261) suffusions. Tail with Grayish Horn Color (268), Sepia (286), and Cream White (52) transversal bands dorsally; Drab (19) laterally; and Smoky White (261) ventrally. Limbs dorsally covered with a reticulation of Drab (19), Chamois (84), and Dusky Brown (285), ventrally grading to Fawn Color (258) in forelimbs, and Ground Cinnamon (270) with suffusions of Smoky White (261) in hind limbs.

Coloration in life. Coloration in life of a young male (SMF 101438) was recorded as follows: Dorsum Mars Brown (223A) with a Tawny Olive (223D) vertebral stripe and transverse lines; dorsum of head Tawny Olive (223D) with a Verona Brown (223B) nuchal band that contains a central Tawny Olive (223D) line; iris Clay Color (123B) with a suffusion of Verona Brown (223B) centrally; dorsal surface of limbs Beige (219D) with Sepia (219) spots; ventral surfaces of head, body and limbs dirty white; dorsal surface of (regenerated) tail light Drab (119C) with scattered Sepia (119) spots; ventral surface of tail Light Drab (119C) with a suffusion of Sepia (119) medially.

Coloration in life of a juvenile female (SMF 101436) was recorded as follows: Dorsal ground color Raw Umber (123) with Raw Umber (223) transverse lines, edged with Pale Horn Color (92) posteriorly. Postocular stripe Ground Cinnamon (239); iris Yellow Ocher (123C) with a suffusion of Dark Drab (119B); dorsal surface of tail Cinnamon Drab (219C) with Sepia (119) bands, borders posteriorly by Chamois (123C); ventral surface of head, body and limbs dirty white, palmar and plantar surfaces Light Drab (119C); anterior portion of ventral tail Beige (219D), with Sepia (119) band on distal portion.

Color variation. One juvenile (SMF 101439, 36 mm SVL) and two young adults (MNHNP 11793, 45 mm SVL; SMF 101438, 45 mm SVL) out of the 17 examined specimens of *Homonota marthae* have a trace of white crescent-shaped band on the occipital area (more visible in the SMF 101439, Fig. 7G), typical of *H. horrida* and *H. septentrionalis*. Nevertheless, many juveniles (such as SMF 101436) show the same coloration as adults (Fig. 7). The specimen MNHNP 7832 has a narrow occipital white band, joined to the postocular lines (Fig. 7C). Some specimens have a darkish coloration (MNHNP 2810, 10744, 11791, 11793) dorsally, and ventrally most of the specimens have a clearer color than the holotype, except for MNHNP 2798, 2810, and 10744. In some specimens (MNHNP 2795, 2798, 2810, 10744) the dorsal color is diffused and the transversal bands are little visible.

Morphological variation. SVL 36–59 mm; TrL 16–27 mm (43.8–48.2% of SVL in females, 40.7–46.7% in males); FL 9–11 mm ($\bar{x}$ 10±0.36) in females, 7–11 mm ($\bar{x}$ 8.7±0.52) in males; TL 8.7–10.1 mm ($\bar{x}$ 9.5±0.2) in females, 8–10.2 mm ($\bar{x}$ 9.1±0.31) in males; AL 9.3–13.7 mm ($\bar{x}$ 12.8±0.28) in females, 11.2–14 mm ($\bar{x}$ 12.4±0.38) in males; HL 9.3–13.8 mm ($\bar{x}$ 13.2±0.19) in females, 11.1–13.5 mm ($\bar{x}$ 12.2±0.31) in males; HW 7.1–11.2 mm (79.4–88% of HL in females, 78.9–85.9% in males); HH 5.5–8.3 mm (52.6–61% of HL in females, 52.6–60.5% in males); END 2.8–5.1 mm (30.8–35.1% of HL in females, 31.4–38.9% in males); ESD 3.9–6.1 mm (40.3–45% of HL in females, 40.5–46.5% in males); EMD 3.1–5 mm (31.3–34.7% of HL in females, 33.8–37% in males); ID 3.8–5.8 mm (33.8–40% of HL in females, 37.1–44.7% in males); IND 1.4–2.1 mm (12.2–16% of HL in females, 11.8–14% in males); SL 5–8; one or two elongated tubercular scales on the mouth commissure; auditory meatus with one large scale on the upper border; IL 5–7; 14–20 longitudinal rows of ventral scales at mid-body; 34–49 transversal rows of ventral scales.

Etymology. This species is named in honor of our indefatigable colleague Martha Motte, who is not only dedicated to safekeeping the herpetological collection of the "Museo Nacional de Historia Natural del Paraguay", but also does a great job in providing selfless support to scientists that are striving to improve the knowledge of the Paraguayan herpetofauna.

Habitat and distribution. *Homonota marthae* is known from the central area of the Paraguayan Dry Chaco in the Department of Boquerón (Fig. 5). The environment is a xeric forest with abundance of thorny vegetation and

almost absence of a herbaceous stratum. Nevertheless, a more detailed analysis of museum collections is advisable for a better knowledge of the distribution of this species.

This species is a dry forest inhabitant, but it is also frequently found in human dwellings. Talbot (1978) recorded the use of logs of Drunken tree (*Chorisia speciosa*: Malvaceae) as shelter by *Homonota* in the Dry Chaco, since the wood of this tree keeps high water levels. Additionally, Cacciali et al. (2007a) demonstrated the use of subterranean caves (usually armadillo burrows) by *Homonota* in several areas of the Paraguayan Chaco.

Discussion

The diversity of species groups within the genus *Homonota* was explored in the last decade, and resulted in the description of *H. williamsii* (Avila et al. 2012) of the *whitii* group, and *H. rupicola* (Cacciali et al. 2007b) and *H. taragui* (Cajade et al. 2013) of the *borellii* group. However, the taxonomy of the *horrida* group (referred to as *fasciata* in Morando et al. 2014) was untouched for many years, and was comprised of two species (*H. horrida* and *H. underwoodi*). Recently, with the description of *H. septentrionalis* by Cacciali et al. (2017), and adding *H. marthae* described herein, the diversity of the *horrida* group currently includes four species. Morando et al. (2014) and Cacciali et al. (2017) presented species trees where the *whitii* group is sister to *horrida* and *borellii* groups. Our deep cluster arrangement is not completely resolved probably due to the use of fewer genes. Nevertheless, there is a strong consensus in the topology of the *horrida* group, where *H. underwoodi* appears as the sister of the remaining taxa (Fig. 1).

No obvious external synapomorphy is known to diagnose the *horrida* group. Three of the four species (*H. horrida*, *H. septentrionalis*, and *H. marthae*) have a pattern characterized by transversal body bands and the presence of a vertebral line. This coloration is different from the remaining species of the genus. The fourth species of the *horrida* group, *H. underwoodi*, has homogeneous body scalation and a completely different pattern, and therefore *H. horrida* and *H. underwoodi* were considered not to be in the same group (Kluge 1964).

The most obvious external difference between *H. marthae* and its presumed closest relative, *H. septentrionalis*, is the lack of a white occipital band in the former taxon, although we found some specimens (mainly juveniles or hatchlings) of *H. marthae* that do have the occipital band. Given that this white occipital band is also present in *H. horrida*, it could be a plesiomorphic character, and therefore the lack of it could be interpreted as the derived state.

Both species seem to inhabit in parapatry the Dry Chaco in Paraguay, and although a major revision of the whole distribution of the group is needed in order to know their actual ranges, *H. septentrionalis* is distributed in the north-westernmost part of the Dry Chaco, whereas *H. marthae* occurs in the central and easternmost areas of the Dry Chaco. Due to the lack of evident geographic barriers between these two species and considering their relatively low morphological variation (especially in males), they remained recognized as a single taxonomic unit until now. Parapatric speciation or breaks to gene flow without evident geographic barriers were observed and discussed by Irwin (2002), and also documented for other geckos in South America's Dry Diagonal, where Werneck et al. (2012) documented a high diversity in sympatric clades of *Phyllopezus* in Caatinga and Cerrado.

The degree of genetic differentiation between these two species is evident, and larger than the degree of morphological differences. Small morphological differentiation or even complete crypsis is common for many organisms, especially when they use the same ecological niche. Specifically for geckos, a recent study showed that it is difficult to find morphological diagnostic characters that match those observed by genetic evidence, as it is the case of the genera *Garthia* and *Homonota*, which are very similar morphologically (Daza et al. 2017). This is in agreement with previous studies that found that molecular genetic tools provided additional evidence for the interpretation of gecko's systematics in the Neotropics (Gamble et al. 2011, Gamble et al. 2012, Morando et al. 2014). The evolutionary processes that led to the molecular differentiation between *H. septentrionalis* and *H. marthae* remain unknown.

Finally, *Homonota marthae* is a common species that resists human perturbation and can be found in rural environments, and although its actual distribution limits are not yet known, and more revisions are needed to target this issue, probably the records of "*Homonota fasciata*" from Defensores del Chaco National Park referred by Cacciali et al. (2016) belong to *H. marthae*, and one of the records of *H. marthae* in Comunidad Ayoreo Tunucojai lays at ~70 km W from Yaguareté Porã Natural Reserve. Thus, we consider that *H. marthae* is not under extinction risk.

Key for identification of the species of the genus *Homonota*

Information to generate the key was based on Cacciali et al. (2007b), Avila et al. (2012), and Cájade et al. (2013). Given that the holotype of *H. fasciata* is completely bleeched, we consider the information on its coloration from the original color description (Duméril and Bibron 1836).

1 Coloration based on irregular or reticulated pattern 2
– Coloration pattern composed of transversal bands 10
2 Dorsal scales homogeneously smooth 3
– Dorsal scales smooth and granular mixed with series of enlarged keeled scales 5

3 Ventral surface of the body immaculate due to lack of chromatophores ..... *H. underwoodi*
– Ventral surface of the body pigmented with chromatophores 4
4 43–49 scales around midbody ..... *H. andicola*
– 55–59 scales around midbody ..... *H. whitii*
5 Series of keeled scales restricted to the posterior half of the dorsum ..... *H. darwinii*
– Series of keeled scales uniformly extended along the whole dorsum 6
6 Dorsal surface of thighs with keeled scales 7
– Dorsal surface of thighs with smooth scales 8
7 Dorsal surface of arms with keeled scales; temporal region with enlarged keeled scales ..... *H. uruguayensis*
– Dorsal surface of arms with smooth cycloid scales; temporal region homogeneously covered by granular scales ..... *H. taragui*
8 146–161 dorsal scales from occipital area to the level of the cloaca; oblique ear opening ..... *H. williamsii*
– 94–139 dorsal scales from occipital area to the level of the cloaca; round ear opening 9
9 45–50 scales around midbody; dorsal surface of the tail with a pattern of thin speckling ..... *H. borellii*
– 54–63 scales around midbody; dorsal surface of the tail with a pattern of black blotches ..... *H. rupicola*
10 Edge of ear opening smooth, without enlarged tubercular scales around; postmentals about five times larger than the scales behind it ..... *H. fasciata*
– Edge of ear opening serrated, with one or two tubercular scales above; postmentals twice larger than the scales behind it 11
11 Tubercles on the dorsal and lateral sides of the neck poorly developed; occipital area with a wide whitish crescent-shaped mark ..... *H. septentrionalis*
– Tubercles on the dorsal and lateral sides of the neck well developed; occipital coloration variable 12
12 Ear opening above the mouth level; occipital area with homogeneous coloration or with a faint reticulation in adults ..... *H. marthae*
– Ear opening at the level of the mouth; occipital area with a wide whitish crescent-shaped mark ..... *H. horrida*

Acknowledgments

Collecting (N° 04/11) and export (N° 02/12) permits were provided by Secretaría del Ambiente. GK thanks Dulcy Vázquez and Thomas and Sabine Vinke for help during fieldwork. We are grateful to Martha Motte (Museo Nacional de Historia Natural del Paraguay - MNHNP) for letting us analyze specimens under her care. For collaboration during collection revisions, we thank Nicolás Martínez (MNHNP) and Cristian F. Pérez (Herpetological collection of the Centro Nacional Patagónico - LJAMM-CNP). We are grateful to the staff (especially Heike Kappes) of the Grunelius-Möllgaard Laboratory (Senckenberg Forschungsinstitut und Naturmuseum Frankfurt - SMF), and to Linda Mogk (SMF) for lab support. PC thanks economic support from the Consejo Nacional de Ciencia y Tecnología (CONACYT, Paraguay) through the Programa Nacional de Incentivo a los Investigadores (PRONII) program. This work is part of an ongoing project of Barcoding of the Paraguayan Herpetofauna, as part of the PhD work of PC, funded by the Deutscher Akademischer Austauschdienst (DAAD, Germany).

References

Abdala V, Lavilla EO (1993) *Homonota fasciata* (Duméril y Bibron, 1836), nombre válido para *Homonota pasteuri* Wermuth, 1965 y *Homonota horrida* (Burmeister, 1861) (Sauria: Gekkonidae). Acta Zoológica Lilloana 42(2): 279–282.

Anisimova M, Gil M, Dufayard JF, Dessimoz C, Gascuel O (2011) Survey of branch support methods demonstrates accuracy, power, and robustness of fast Likelihood-based approximation schemes. Systematic Biology 60(5): 685–699. https://doi.org/10.1093/sysbio/syr041

Avila LJ, Pérez CHF, Minoli I, Morando M (2012) A new species of *Homonota* (Reptilia: Squamata: Gekkota: Phyllodactilidae) from the Ventania mountain range, Southeastern Pampas, Buenos Aires Province, Argentina. Zootaxa 3431: 19–36. http://www.mapress.com/j/zt/article/view/13976

Bouckaert RR, Heled J (2014) DensiTree 2: seeing trees through the forest. bioRxiv, http://dx.doi.org/10.1101/012401

Burmeister H (1861) Reise durch die La Plata Staaten mit besonderer Rücksicht auf die physische Beschaffenheit und den Culturzustand der Argentinischen Republik. Ausgeführt in den Jahren 1857, 1858, 1859 und 1860. H.W. Schmidt, Halle, 515 pp. https://archive.org/details/bub_br_1918_00361310

Cacciali P, Brusquetti F, Bauer F, Sánchez H (2007a) Contribuciones al conocimiento de la biología de *Homonota fasciata* (Sauria: Gekkonidae) en el Chaco paraguayo. Boletín de la Asociación Herpetológica Española 18: 73–77.

Cacciali P, Ávila I, Bauer F (2007b) A new species of *Homonota* (Squamata, Gekkonidae) from Paraguay, with a key to the genus. Phyllomedusa 6(2): 137–146. http://dx.doi.org/10.11606/issn.2316-9079.v6i2p137-146

Cacciali P, Scott NJ, Aquino Ortíz AL, Fitzgerald LA, Smith P (2016) The Reptiles of Paraguay: literature, distribution, and an annotated taxonomic checklist. Special Publications of the Museum of Southwestern Biology 11: 1–373. http://digitalrepository.unm.edu/msb_special_publications/1/

Cacciali P, Morando M, Medina CD, Köhler G, Motte M, Avila LJ (2017) Taxonomic analysis of Paraguayan samples of *Homonota fasciata* Duméril & Bibron (1836) with the revalidation of *Homonota horrida* Burmeister (1861) (Reptilia: Squamata: Phyllodactylidae) and the description of a new species. PeerJ 5: e3523. http://dx.doi.org/10.7717/peerj.3523

Cajade R, Etchepare EG, Falcione C, Barraso DA, Álvarez BB (2013) A new species of *Homonota* (Reptilia: Squamata: Gekkota: Phyllodactylidae) endemic to the hills of Paraje Tres Cerros, Corrientes Province, Argentina. Zootaxa 3709(2): 162–176. http://dx.doi.org/10.11646/zootaxa.3709.2.4.

Carreira S, Meneghel M, Achaval F (2005) Reptiles de Uruguay. Universidad de la República, Montevideo, 639 pp.

Cei JM (1993) Reptiles del noroeste, nordeste y este de la Argentina. Herpetofauna de las selvas subtropicales, Puna y Pampas. Museo Regionale di Scienze Naturali Monografie 14: 1–949.

Corl A, Davis AR, Kuchta SR, Comendant T, Sinervo B (2010) Alternative mating strategies and the evolution of sexual size dimorphism in the side-blotched lizard, *Uta stansburiana*: a population-level comparative analysis. Evolution, 64(1): 79–96. http://dx.doi.org/10.1111/j.1558-5646.2009.00791.x

Daza JD, Gamble T, Abdala V, Bauer AM (2017) Cool geckos: does plesiomorphy explain morphological similarities between geckos from the southern cone? Journal of Herpetology 51(3): 330–342. https://doi.org/10.1670/16-162

Drummond AJ, Suchard MA, Xie D, Rambaut A (2012) Bayesian phylogenetics with BEAUti and the BEAST 1.7. Molecular Biology and Evolution 29: 1969–1973. https://doi.org/10.1093/molbev/mss075

Duméril AMC, Bibron G (1836) Erpetologie générale ou histoire naturelle complete des reptiles. Vol. 3. Libr. Encyclopédique Roret, Paris, 517 pp. https://www.biodiversitylibrary.org/item/99518#page/9/mode/1up

Gamble T, Bauer AM, Colli GR, Greenbaum E, Jackman TR, Vitt LJ, Simons AM (2011) Coming to America: multiple origins of New World geckos. Journal of Evolutionary Biology 24(2): 231–244. http://dx.doi.org/10.1111/j.1420-9101.2010.02184.x

Gamble T, Colli GR, Rodrigues MT, Werneck FP, Simons AW (2012) Phylogeny and cryptic diversity in geckos (*Phyllopezus*; Phyllodactylidae; Gekkota) from South America's open biomes. Molecular Phylogenetics and Evolution 62(3): 943–953. https://doi.org/10.1016/j.ympev.2011.11.033

Gelman A, Rubin DB (1992) Inference from Iterative Simulation Using Multiple Sequences. Statistical Science 7: 457–511. https://doi.org/10.1214/ss/1177011136

Glez-Peña D, Gómez-Blanco D, Reboiro-Jato M, Fdez-Riverola F, Posada D (2010) ALTER: program-oriented conversion of DNA and protein alignments. Nucleic Acid Research 38: W14–W18. https://doi.org/10.1093/nar/gkq321

Guindon S, Dufayard JF, Lefort V, Anisimova M, Hordijk W, Gascuel O (2010) New algorithms and methods to estimate maximum-likelihood phylogenies: assessing the performance of PhyML 3.0. Systematic Biology 59(3): 307–321. https://doi.org/10.1093/sysbio/syq010

Hammer Ø, Happer DAT, Ryan PD (2001) PAST: Paleontological Statistics software package for education and data analysis. Paleontologica Electronica 4: 9. http://palaeo-electronica.org/2001_1/past/issue1_01.htm

Huelsenbeck JP, Ronquist F (2001) Mrbayes: Bayesian inference of phylogeny. Bioinformatics 17(8): 754–755. https://doi.org/10.1093/bioinformatics/17.8.754

Irwin DE (2002) Phylogeographic breaks without geographic barriers to gene flow. Evolution 56: 2383–2394. https://doi.org/10.1111/j.0014-3820.2002.tb00164.x

Jarvis A, Reuter HI, Nelson A, Guevara E (2008) Hole-filled SRTM for the globe Version 4, available from the CGIARCSI SRTM 90m. http://srtm.csi.cgiar.org. [Accessed 02 February 2015]

Katoh K, Standley DM (2013) MAFFT multiple sequence alignment software version 7: improvements in performance and usability. Molecular Biology and Evolution 30(4): 772–780. https://doi.org/10.1093/molbev/mst010

Katoh K, Toh H (2008) Improved accuracy of multiple ncRNA alignment by incorporating structural information into a MAFFT-based framework. BMC Bioinformatics 9: 212. https://doi.org/10.1186/1471-2105-9-212

Kekkonen M, Mutanen M, Kaila L, Nieminen M, Hebert PDN (2015) Delineating species with DNA barcodes: a case of taxon dependent method performance in moths. PLoS ONE 10: e0122481. https://doi.org/10.1371/journal.pone.0122481

Kluge AG (1964) A revision of the South American gekkonid lizard genus *Homonota* Gray. American Museum Novitates 2193: 1–41 .

Köhler G (2012) Color Catalogue for Field Biologists. Herpeton, Offenbach, 49 pp.

Köhler G (2014) Characters of external morphology used in *Anolis* taxonomy—Definition of terms, advice on usage, and illustrated examples. Zootaxa 3774: 201–257. http://dx.doi.org/10.11646/zootaxa.3774.3.1

Lanfear R, Frandsen PB, Wright AM, Senfeld T, Calcott B (2016) PartitionFinder 2: new methods for selecting partitioned models of evolution formolecular and morphological phylogenetic analyses. Molecular Biology and Evolution 34(3): 773–773. https://doi.org/10.1093/molbev/msw260

Mayrose I, Friedman N, Pupko T (2005) A Gamma mixture model better accounts for among site rate heterogeneity. Bioinformatics 21: 151–158. https://doi.org/10.1093/bioinformatics/bti1125

Minh BQ, Thi Nguyen MA, von Haeseler A (2013) Ultrafast approximation for phylogenetic bootstrap. Molecular Biology and Evolution 30(5): 1188–1195. http://dx.doi.org/10.1093/molbev/mst024

Morando M, Medina CD, Ávila LJ, Pérez CHF, Buxton A, Sites JW (2014) Molecular phylogeny of the New World gecko genus *Homonota* (Squamata: Phyllodactylidae). Zoologica Scripta 43(3): 249–260. https://doi.org/10.1111/zsc.12052

Nguyen LT, Schmidt HA, von Haeseler A, Minh BQ (2015) IQ-TREE: A fast and effective stochastic algorithm for estimating Maximum Likelihood phylogenies. Molecular Biology and Evolution 32(1): 268–274. http://dx.doi.org/10.1093/molbev/msu300

Ogilvie HA, Bouckaert RR, Drummond AJ (2017) StarBEAST2 brings faster species tree inference and accurate estimates of substitution rates. Molecular Biology and Evolution 34: 2101–2114. http://dx.doi.org/10.1093/molbev/msx126

Prado DE, Gibbs PE (1993) Patterns of species distributions in the Dry Seasonal Forest of South America. Annals of Missouri Botanical Garden 80(4): 902–927. https://doi.org/10.2307/2399937

Puillandre N, Lambert A, Broullet S, Achaz G (2012) ABGD, Automatic Barcode Gap Discovery for primary species delimitation. Molecular Ecology 21(8): 1864–1877. http://dx.doi.org/10.1111/j.1365-294X.2011.05239.x

Ronquist F, Huelsenbeck JP (2003) MrBayes version 3: Bayesian phylogenetic inference under mixed models. Bioinformatics 19(12): 1572–1574. https://doi.org/10.1093/bioinformatics/btg180

Shapiro SS, Wilk MB, Chen H (1968) A comparative study of various tests of normality. Journal of the American Statistical Association 63(324): 1343–1372. https://doi.org/10.2307/2285889

Smithe FB (1981) Naturalist's Color Guide. Part I. American Museum of Natural History, New York, 23 pp.

Stucky BJ (2012) SeqTrace: A graphical tool for rapidly processing DNA sequencing chromatograms. Journal of Biomolecular Techniques 23(3): 90–93. https://doi.org/10.7171/jbt.12-2303-004

Sullivan J, Swofford DL, Naylor GJP (1999) The effect of taxon sampling on estimating rate heterogeneity parameters of maximum-likelihood models. Molecular Biology and Evolution 16: 1347–1356. https://doi.org/10.1093/oxfordjournals.molbev.a026045

Surget-Groba Y, Thorpe RS (2013) A likelihood framework analysis of an island radiation: phylogeography of the Lesser Antillean gecko *Sphaerodactylus vincenti*, in comparison with the anole *Anolis roquet*. Journal of Biogeography 40(1): 105-116. https://doi.org/10.1111/j.1365-2699.2012.02778.x

Talbot JJ (1978) Ecological notes on the Paraguayan Chaco herpetofauna. Journal of Herpetology 12: 433-435. https://doi.org/10.2307/1563636

Trifinopoulos J, Nguyen LT, von Haeseler A, Minh BQ (2016) W-IQ-TREE: a fast online phylogenetic tool for Maximum Likelihood analysis. Nucleic Acid Research 44: W232–W235. https://doi.org/10.1093/nar/gkw256

Werneck FP, Gamble T, Colli GR, Rodrigues MT, Sites J (2012) Deep diversification and long-term persistence in the South American "Dry Diagonal": integrating continent-wide phylogeography and distribution modeling of geckos. Evolution 66: 3014–34. https://doi.org/10.1111/j.1558-5646.2012.01682.x

Yachdav G, Wilzbach S, Rauscher B, Sheridan R, Sillitoe I, Procter J, Lewis SE, Rost B, Goldberg T (2016) MSAViewer: interactive JavaScript visualization of multiple sequence alignments. Bioinformatics 32(22): 3501–3503. https://doi.org/10.1093/bioinformatics/btw474

Yang Z, Landry JF, Hebert PDN (2016) A DNA Barcode Library for North American Pyraustinae (Lepidoptera: Pyraloidea: Crambidae). PLoS ONE 11: e0161449. https://doi.org/10.1371/journal.pone.0161449

Zar J (1999) Biostatistical Analysis, 4th ed. Prentice-Hall, New Jersey, 929 pp.

Appendix 1

Examined specimens

Homonota horrida

ARGENTINA: La Pampa: Ruta Provincial 1, 23.6 km W from intersection with Ruta Nacional 151 (LJAMM-CNP 10523, 10584); Ruta Provincial 27, 37.7 km S from intersection with Ruta Provincial 14 (LJAMM-CNP 10578–9). Mendoza: 1 km S Punta de Agua (LJAMM-CNP 10493, 10496, 10576–7). Neuquén: 41 km NW Punta Carranza (LJAMM-CNP 8713); 6 km SW Picun Leufu (LJAMM-CNP 13948); Ruta Provinicial 5, 10 km N from Ruta Provincial 7 (LJAMM-CNP 7804); Mina La Casualidad (LJAMM-CNP 14551); Villa El Chocón (LJAMM-CNP 6967–8). Río Negro: Avellaneda (LJAMM-CNP 7670, 7674); Villa Regina (LJAMM-CNP 6520, 6530, 6532–3, 6535).

Homonota septentrionalis

PARAGUAY: Boquerón: Cruce San Miguel (MNHNP 11850, 11855, 11860, 11872); Fortín Mayor Infante Rivarola (MNHNP 12238, SMF 101984); Parque Nacional Teniente Enciso (MNHNP 2821, 9037–8, 9131, 11410, 11421, 11423).

Acronyms

LJAMM-CNP: Colección de herpetología del Centro Nacional Patagónico.

MNHNP: Museo Nacional de Historia Natural del Paraguay.

SMF: Senckenberg Forschungsinstitut und Naturmuseum Frankfurt.

Supplementary material 1

Supplementary information

Authors: Pier Cacciali, Mariana Morando, Luciano J. Avila, Gunther Köhler

Data type: Adobe PDF file

Explanation note: Description of a new species of Homonota (Reptilia, Squamata, Phyllodactylidae) from the central region of northern Paraguay

Link: https://doi.org/10.3897/zse.94.21754.suppl1